STUDY OF THE INTERLAMINAR QUASI-STATIC AND FATIGUE BEHAVIOUR OF A CARBON PPS USING THE SINGLE LAPSHEAR GEOMETRY

I. De Baere[a*], W. Van Paepegem[a], J. Degrieck[a]

[a]*Mechanics of Materials and Structures, Department of Materials Science and Engineering, Ghent University, Technologiepark-Zwijnaarde 903, 9052 Zwijnaarde, Belgium*
**Ives.DeBaere@UGent.be*

Keywords: Benchmark, Experimental, Thermoplastic, Joints

Abstract
Although fusion bonded joints have already been extensively studied, they are only rarely compared to benchmark specimens with the same interlaminar behaviour of the composite material being joined, especially for the lapshear geometry. In this manuscript, a method of producing such benchmark lapshear specimens is presented for a hot pressed carbon fabric reinforced thermoplastic. The mechanical behaviour of these specimens is then assessed using quasi-static and tension-tension fatigue experiments. No crack growth was visible during the quasi-static experiments, except near the very end of life, whereas significant crack growth was present during fatigue experiments.

1. Introduction

The study presented here fits within a broader research project on the mechanical behaviour of fusion bonded joints between carbon fibre 5-harness satin weave reinforced polyphenylene sulphide (PPS) composite specimens. The optimization of the welding parameters of this infrared welding was already published in [1], where the results of single lapshear experiments were used for the assessment of quality and reproducibility of the joints. To obtain a benchmark for the welded joints to be compared with, a second study was conducted [2] where the interlaminar behaviour under pure mode I and pure mode II was investigated; values for G_I and G_{II} were also determined, both for initiation and propagation.

Prior to going to fatigue lapshear experiments on the welded joints, it was decided that it would be useful to again have a benchmark for the lapshear behaviour of the base material. Therefore, the emphasis of this manuscript lies on determining the mechanical behaviour of the carbon PPS under study for a lapshear specimen, where the shear loaded overlap has the exact same properties of the standard hot pressed plates, as for these, the production process has been optimised and should therefore yield the best interlaminar behaviour achievable. Although different fusion bonding processes have already been extensively studied, as illustrated in various review articles [3, 4], the comparison between a benchmark and the welds is only rarely considered [5, 6, 7]. For these studies, benchmark or reference specimens are mentioned, but not much detail is provided. Usually, only lapshear strength values are listed in a table, but detailed information and images on the production method are not given. Moreover, only the quasi-static behaviour is considered.

To obtain a lapshear geometry with the optimal properties, some possibilities are already considered in the mentioned literature. Developing a hot pressing mould for this geometry, which was considered in [5] not only is difficult and expensive, it would also mean that a different mould is needed for other material types, or other overlap lengths. In [6], an autoclaved reference is mentioned, but no further details on the process, for instance on how to obtain straight edges on the overlap are given. In [7], a plate of sufficient thickness is considered, after which the unnecessary material is removed by machining and grinding, but again, no further details, for instance on surface and edge quality, or the occurrence of delaminations due to the machining are provided. The method presented in this paper also uses the principle of removing excess material, but with only limited machining.

2. Materials and methods

The composite material used for the experiments was a 5-harness satin-weave carbon fabric-reinforced polyphenylene sulphide (PPS). The carbon PPS plates were hot pressed, one stacking sequence was used for this study, namely $[(0^o,90^o)_{4s}]_s$ where (0º,90º) represents one layer of fabric. The choice for this stacking sequence was driven by the fact that the experiments in this manuscript will serve as benchmark for the welded specimens, which also have this stacking sequence in their welded overlap [1]. The in-plane elastic properties and the tensile strength properties are listed in Table 1. This material was supplied to us by Ten Cate Advanced Composites (The Netherlands).

E_{11} [GPa]	E_{22} [GPa]	ν_{12} [-]	G_{12} [GPa]	X_T [MPa]	ε_{11}^{ult} [-]	Y_T [MPa]	ε_{22}^{ult} [-]	S_T [MPa]
56.0	57.0	0.033	4.175	736	0.011	754.0	0.013	110.0

Table 1 Elastic and strength properties of the CETEX® material

The desired geometry of the single lapshear specimen is illustrated in Figure 1 and is chosen according to the ASTM D5868-01 '*Standard Test Method for Lap Shear Adhesion for Fiber Reinforced Plastic Bonding*', which was also considered for [1]; the width of the specimen is 25 mm.

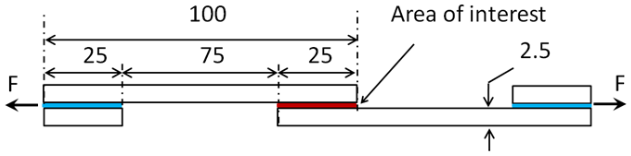

Figure 1 Single-lapshear geometry; dimensions in mm.

All tensile tests were performed on a servo-hydraulic INSTRON 8801 tensile testing machine with a FastTrack 8800 digital controller and a load cell of ±100kN. The quasi-static tests were displacement-controlled at a displacement speed of 0.5mm/min, whereas the fatigue experiments were done in load-control. For the registration of the tensile data, a combination of a National Instruments USB 6251 data acquisition card and the SCB-68 pin shielded connector were used. The load F and displacement δ, given by the FastTrack controller were sampled on the same time basis.

For the test specimen preparation, the idea was to produce a larger plate with the same stacking sequence of the welded overlaps in [1], and then to trim away all unwanted parts to obtain the desired lapshear geometry. By doing so, the overlap of the lapshear specimen is produced using the optimal process parameters for the standard plates. However, as it is not the purpose to induce a significant amount of damage by milling away all unnecessary material, thus corrupting the experimental data, a kapton film of 50 micron was carefully inserted on strategic places, so that four cuts with a diamond disc suffice to obtain the lapshear geometry; Teflon film was not an option, because the processing temperature of the carbon-PPS exceeds the maximum service temperature of Teflon films. Figure 2 illustrates the cutting process.

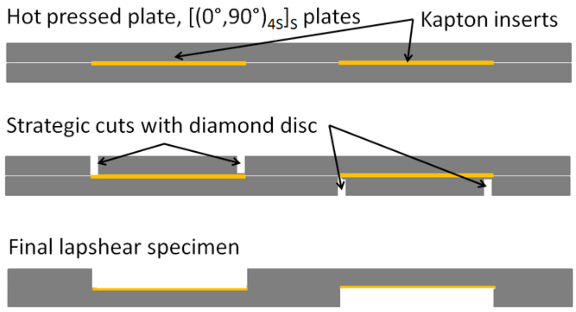

Figure 2 Illustration of the cutting of the single-lapshear geometry.

After hot pressing, the sides were examined using a microscope and the exact position of the kapton film was marked. Then, the cuts were made, making sure that they were just as deep as the kapton film. Finally, the excess parts are removed. The cut should have the exact depth to have the correct lapshear geometry on the microscopic level (meaning a fairly straight angle), since otherwise unwanted stress concentrations could arise which will influence crack initiation, both under static and fatigue loading conditions [8, 9]. However, if the described process is done very carefully, then nice straight angles can be obtained and no delaminations are induced. For all specimens documented in this manuscript, it was first confirmed microscopically that a nice cut at the correct depth was achieved and that no delaminations due to the cutting were present. The length of the overlap was 25.0 ± 0.5 mm for all specimens.

3. Experiments and Discussion

3.1. Quasi-static experiments

The first concern was of course to verify whether reproducible results were achieved with the proposed method of generating specimens. As such, a large amount of specimens were generated and tested. Figure 3 illustrates a few of the results from the specimens with the correct geometry and as can be seen, reproducible results are obtained. There is a little scatter on the stiffness of the lapshear joint, but this is due to the small differences in overlap, as was validated by finite element modeling, which is not discussed here. An averaged failure load of

17.7 MPa ± 0.4 MPa was obtained from all experiments. For clarity's sake, the different curves are given an offset along the displacement-axis.

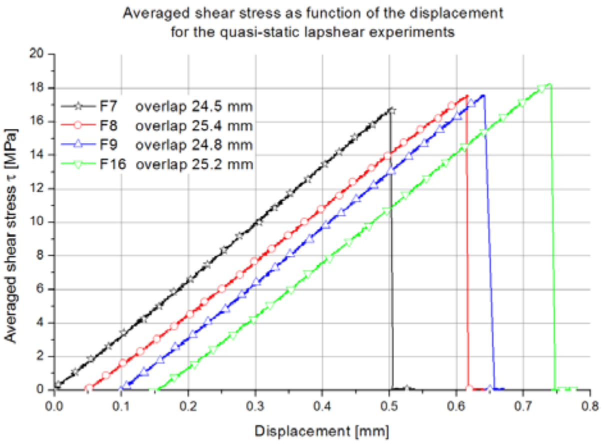

Figure 3 Results for the quasi-static lapshear experiments

To assess the origin and propagation of the crack, a number of specimens where polished and with a travelling microscope, the edge of the overlap was observed. Figure 4 illustrates the pictures taken during the experiment on sample F16, pictures were taken every 500 N and at failure, but only the significant ones are shown here. Besides bending of the specimen, nothing was really noticeable until 9 kN was reached. Between 9 kN and 10 kN a small change in color (whitening of the area) could be distinguished in the corner of the lapshear, hinting that a crack tip was initiating. This crack tip could be distinguished in the picture of 10.5 kN (Figure 4 (a)). At 11 kN, this crack is more clearly visible and has a length of about 0.6 mm at the polished side; 100 N later, this resulted in final failure of the specimen. Similar observations were made for other specimens.

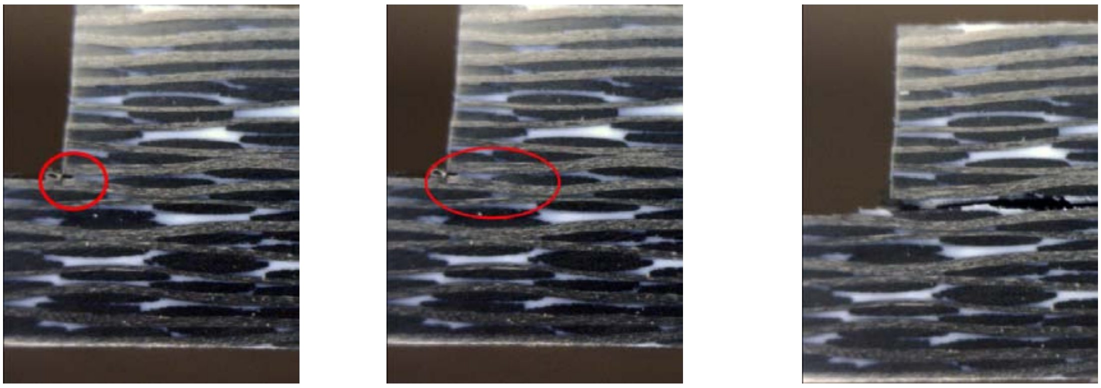

(a) At 10.5 kN (τ=16.7 MPa) (b) At 11 kN (τ=17.5 MPa) (c) Failure at 11.1kN (τ=17,6 MPa)

Figure 4 Microscopic images of a quasi-static lapshear test.

As such, it can be concluded that there is virtually no crack growth present before final failure.

3.2. Tension-tension fatigue experiments

Finally, fatigue experiments were performed. As previously mentioned, all tests were done in load control and to avoid buckling, the minimum load was set at 0.2 kN. The maximum load was chosen as a percentage of the average quasi-static failure load and to verify whether a frequency dependency was present, tests were done both at 2 Hz and 5 Hz loading frequency. To observe what is happening during the fatigue, every five minutes, four fatigue cycles were registered and the minimum, maximum and mean value of the signals was stored. Figure 5 (a) gives an overview of the experiments and it can be noted that the scatter is quite low for these results. Furthermore, there is no frequency dependency.

To have a first idea of what is happening during the fatigue life, the displacement of the specimen is observed using the maximum, minimum and mean values of the measurement. As the tests were done in load control, an idea on possible permanent elongation, as well as stiffness degradation can be given. Figure 5 (b) illustrates the evolution of the displacement for one of the experiments at 2Hz at 60% of the quasi-static strength (τ^{max} = 10.6 MPa). It should be mentioned that a similar behaviour was found for all experiments, regardless the maximum load level and the loading frequency.

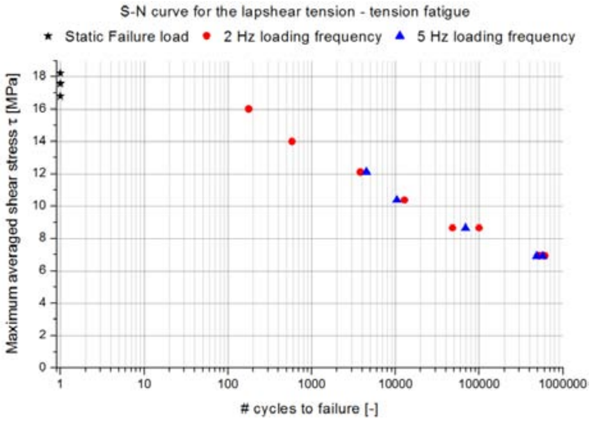

(a) Overview of τ^{max} as function of # cycles till failure

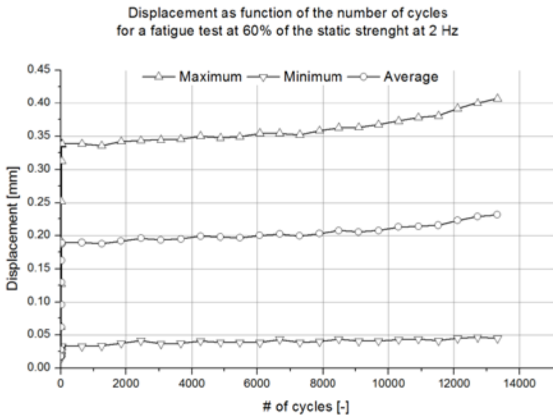

(b) Max., min., and mean value of the displacement for a fatigue test.

Figure 5 Illustration of some fatigue results

From these evolutions, two important conclusions can be drawn. As the minimum of the displacement does not increase, there is no permanent deformation. Given the low uni-axial load levels, no permanent deformation of the adherents was expected, but this means that there is virtually no permanent deformation of the overlap area under shear loads. A little sliding of the specimen in the grips is present, as can be seen at the beginning of the test since the displacement starts at 0 mm, but increases slightly. Second, the difference between the maximum and the minimum displacement increases throughout the experiment. This means that the longitudinal stiffness of the specimen decreases and the rate of decrease, increases with increasing number of cycles. This stiffness decrease suggests crack growth during fatigue life.

To have an idea of the crack growth, again polished samples were tested and the sides were observed using a travelling microscope. To have an idea of the longitudinal stiffness, every x number of cycles, a quasi-static experiment was done, similar to those in section 3.1 and microscopic pictures were taken during these static tests. For these tests, it was noticed that there was virtually no permanent elongation, only small slippage occured during the first test. The slope did not change significantly during the first 20 000 cycles, but it could clearly be noted that the curve for 30 000 and certainly for 40 000 has a lower slope. The specimen failed after 48 229 cycles. Figure 6 illustrates the microscopic pictures, taken during the intermediate quasi-static tests, at maximum load of the static test, which of course did not exceed the maximum load during the fatigue experiment so no extra damage is generated. As such, the crack opens up due to the inherent bending and the crack is more easily visualized. On the images, the actual crack, meaning where there is no longer contact between the crack fronts, is highlighted with a red line. For pictures (c) and (d), it can be seen that the crack initially follows the warp yarns (0°) of the layer (c), but then jumps again to the mid-plane (d). At final failure, the crack indeed propagated in the central plane of the specimen; occasionally, some of the weft yarns (90°) were pulled out.

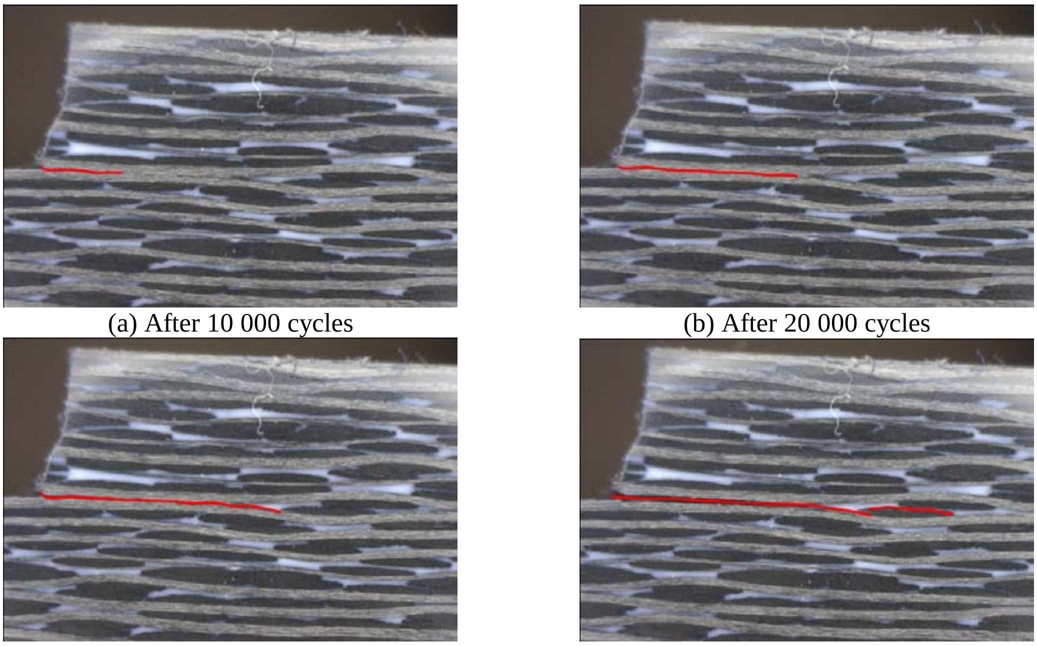

(a) After 10 000 cycles　　(b) After 20 000 cycles

(c) After 30 000 cycles　　(d) After 40 000 cycles

Figure 6 Overview of microscopic assessment of the crack growth during a fatigue experiment; pictures taken at maximum load.

As previously mentioned, given the fact that the fatigue tests are done in load control, the difference between maximum and minimum displacement yield information on the overall stiffness of the specimen. If this is visualized in another way, however, an interesting phenomenon arises. Consider the relative change in stiffness k_{rel}^{N} after a certain number of cycles N, calculated by Equation (1):

$$k_{rel}^{N} = \frac{k_N}{k_{ini}} = \frac{\dfrac{\tau_{\max} - \tau_{\min}}{d_{\max,N} - d_{\min,N}}}{\dfrac{\tau_{\max} - \tau_{\min}}{d_{\max,ini} - d_{\min,ini}}} = \frac{d_{\max,ini} - d_{\min,ini}}{d_{\max,N} - d_{\min,N}} \tag{1}$$

Where $\tau_{\max} - \tau_{\min}$ = average shear stress amplitude, which is constant (load control)

$d_{(min/max), N}$ = maximum or minimum displacement after N cycles
$d_{(min/max), ini}$ = maximum or minimum displacement just after run-in of the test

By using the displacement amplitude after the run-in of the test, the effect of slippage in and further tightening of the grips is ruled out. If this parameter is plotted against the relative time N/N_f with N_f the number of cycles till failure, then this yields Figure 7, where a representative of every load level and frequency is plotted. It was verified for all tests that a similar overlapping curve was found; only one is plotted here for clarity's sake.

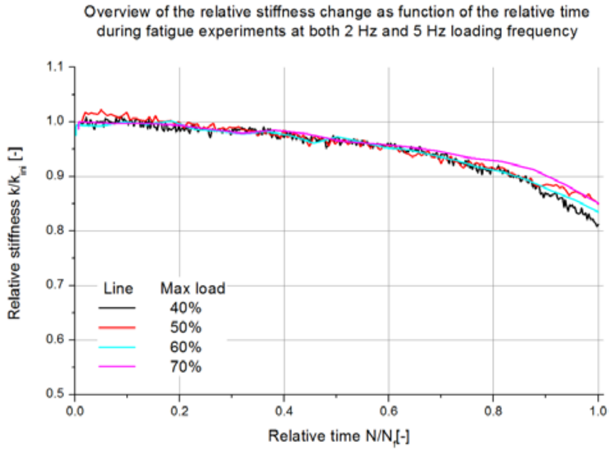

Figure 7 Illustration of the relative decrease in slope as function of relative fatigue life.

It is important to note that almost exactly the same curve is achieved, regardless of the loading frequency or maximum load level. As there was no influence of the frequency on the fatigue life, it is quite fair to assume that the frequency again has no influence in this case. The fact that the load level also has no influence is due to the fact that results from different load levels are compared to different initial slopes. Indeed, due to the implicit bending of the lapshear adherents, the force-displacement curve is non-linear and shows an increasing slope. The fact that Figure 7 shows some sort of 'fatigue master curve', is in fact not that complicated to explain, since it is another way of visualizing Paris' law for crack growth. The main advantage of working with the relative stiffness of the specimen is that there is no need to measure the crack length in order to determine the remaining fatigue life. Only the stiffness of the undamaged specimen at the start of the test and the current stiffness and number of cycles suffices to determine where exactly the test is on the master curve and the remaining fatigue life can be estimated.

4. Conclusions

In this manuscript, the interlaminar behaviour of a 5 harness carbon fabric reinforced polyphenylene sulphide was examined using lapshear experiments, with a geometry according to the ASTM D5868-01. This geometry was derived from hot pressed plates, by removing the excess material in order to obtain this geometry, thus yielding a lapshear overlap with the exact same interlaminar properties as standard hot pressed plates. Quasi-static and fatigue loading conditions were considered and the influence on force-displacement relationship, crack growth and fatigue behaviour was observed.

Taking the production method for obtaining the specimens into account, it could be concluded that reproducibility was very high under both loading conditions. It was found that under quasi-static loading, there was virtually no crack growth and only just before final, brittle failure, a small crack could be distinguished on the polished sides of the specimen. For fatigue loads, however, crack growth could very clearly be seen, even very early in fatigue life. Two loading frequencies were considered, however no significant influence on the behaviour and lifetime could be observed. When plotting the relative stiffness of the entire specimen as a function of the relative fatigue life, a 'master curve' which was the same, regardless of maximum load level or frequency, could be derived. This master curve in fact gives similar information as Paris' law and thus also allows predicting remaining lifetime, but without the need of measuring the crack length.

5. Acknowledgements

The authors are highly indebted to the Fund of Scientific Research – Flanders (F.W.O.) for sponsoring this research and to Ten Cate Advanced Composites for supplying the material.

References

[1] De Baere I., Allaer, K., Jacques S., Van Paepegem W. and Degrieck J. Study of the interlaminar behavior of infrared welded joints of carbon fabric reinforced polyphenylene sulphide. *Polymer Composites* 33 (7):1105-1113, 2012

[2] De Baere I., Jacques S., Van Paepegem W. and Degrieck J. Study of the Mode I and Mode II interlaminar behavior of a carbon fabric reinforced thermoplastic. *Polymer Testing* 31(2):322 – 332, 2012

[3] Stavrov D, Bersee H. Resistance welding of thermoplastic composites - an overview. *Composites Part A-Applied Science and Manufacturing* 36 (1): 39-54, 2005

[4] Yousefpour A, Hojjati M, Immarigeon JP. Fusion bonding/welding of thermoplastic composites. *Journal of Thermoplastic Composite Materials* 17 (4): 303-341, 2004.

[5] Hou M, Ye L, Mai YW. An experimental study of resistance welding of carbon fibre fabric reinforced polyetherimide (CF fabric PEI) composite material. *Applied Composite Materials* 6 (1): 35-49, 1999.

[6] W. Suwanwatana, S. Yarlagadda and J.W. Gillespie, Jr. Hysteresis heating based induction bonding of thermoplastic composites. *Composites Science and Technology* 66 (11-12): 1713-1723, 2006.

[7] Ageorges C, Ye L, Hou M. Experimental investigation of the resistance welding of thermoplastic-matrix composites. Part II: optimum processing window and mechanical performance. *Composites Science and Technology* 60 (8): 1191-1202, 2000.

[8] Quaresimin M, Ricotta M. Stress intensity factors and strain energy release rates in single lap bonded joints in composite materials. *Composites Science and Technology* 66 (5): 647-656, 2006.

[9] Wang, Z.Y., L. Wang, W. Guo, H. Deng, J.W. Tong, and F. Aymerich, An investigation on strain/stress distribution around the overlap end of laminated composite single-lap joints. *Composite Structures* 89(4): 589-595, 2009.